Design of a strong X-Y coupling beam transport line for J-PARC muon g-2/EDM experiment

H. Iinuma, H. Nakayama, M. Abe, K. Sasaki and T. Mibe

***Abstract*—A strategy to design of a dedicated beam transport line for J-PARC Muon g-2/EDM experiment is described. To accomplish three-dimensional beam injection into the MRI-type compact storage ling, transverse beam phase spaces (X and Y components) should be coupled appropriately. We introduce a X-Y coupling, extended Twiss-parameters, and transfer-matrix of the entire transport line. We also discuss about detailed parameters of rotating quadruple magnets along the transport line.**

***Index Terms*—Three-dimensional spiral injection, X-Y coupling, Rotating quadruples.**

I. Introduction

A NEW measurement of the muon's anomalous magnetic moment $a_\mu = (g-2)/2$ and its electric dipole moment (EDM) is in preparation in J-PARC muon facility at MLF, MUSE[1]. These physics quantities are good probes to explore the beyond the standard model in elementary physics. Experimentally, we measure them from a difference of two angular frequencies of spin precession frequency ω_s and orbital cyclotron precession frequency ω_c in a homogeneous magnetic field as shown in Fig. 1.

Two dipole moment of the muon are introduced:

$$\begin{aligned} \vec{\mu}_\mu &= -\frac{gq}{2m}\vec{s}, \\ \vec{d}_\mu &= \eta\frac{q}{2mc}\vec{s}. \end{aligned} \tag{1}$$

Here, c and q are the speed of light and a unit charge, m and g are mass and gyro-magnetic ratio of the muon, respectively. The first equation express a muon magnetic moment. The second is an electric dipole moment, η in Eq. 1 is required to be extremely small from the standard model. If we assume non-zero η here, but assuming that $\vec{\beta}\cdot\vec{B} = \vec{\beta}\cdot\vec{E} = 0$, a muon spin precession frequency is written as:

$$\begin{aligned} \vec{\omega}_a &= \vec{\omega}_s - \vec{\omega}_c \\ &= -\frac{q}{mc}\left[a_\mu\vec{B} - \left(a_\mu - \frac{1}{\gamma^2-1}\right)\vec{\beta}\times\frac{\vec{E}}{c}\right. \\ &\quad \left. +\frac{\eta}{2}\left(\vec{\beta}\times\vec{B} + \frac{\vec{E}}{c}\right)\right]. \end{aligned} \tag{2}$$

In the case of no electric field ($\vec{E}=0$), Equation 2 becomes:

$$\vec{\omega}_a = -\frac{q}{m}a_\mu\vec{B} + \frac{\eta}{2}\left(\vec{\beta}\times\vec{B}\right) \tag{3}$$

This work was supported by JSPS KAKENHI(19H00673). H.Iinuma is with Ibaraki University, Japan (e-mail:hiromi.iinuma.spin@vc.ibaraki.ac.jp). M. Abe, K. Sasaki, H. Nakayama and T. Mibe are with High Energy Accelerator Research Organization (KEK), Tsukuba, Japan.

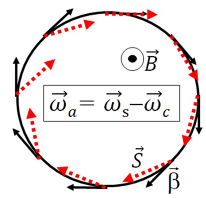

Fig. 1. Definition of spin precession frequency.

We should note that the first and the second terms in Eq. 3 are **orthogonal** to each other. Therefore, precession vector $\vec{\omega}_a$ has a tilt angle against the magnetic field $\vec{B}$. This tilt angle is proportional to the magnitude of EDM and of the order of 1 mrad, if we take the upper limit from the previous experiment E821 [2] ($|\vec{d}_\mu| = 0.9\times10^{-19}$ $e\cdot$cm). To achieve 100 times better sensitivity, we should be sensitive down to 0.01 mrad. Three important points to accomplish Eq. 3 for the new experiment at J-PARC are:

i Electric field should be negligibly small,
ii $\vec{B}$ is precisely adjusted 1 ppm locally and 0.1 ppm averaged along the orbit,
iii An average of outer product of $\vec{\beta}$ and $\vec{B}$ should be smaller than 10^{-5} to achieve a sensitivity of $|\vec{d}_\mu|$ of the order of 10^{-21} $e\cdot$cm.

II. The muon storage magnet

In J-PARC, a slow muons source and a muon LINAC technologies have been developed [1] to have a very low emittance muon beam of momentum of 300 MeV/c. Then muons are stored into a 3 T MRI-type solenoid magnet as shown in Fig. 2. We would emphasize that a diameter of the orbital cyclotron motion becomes **only** 0.66 m. This is

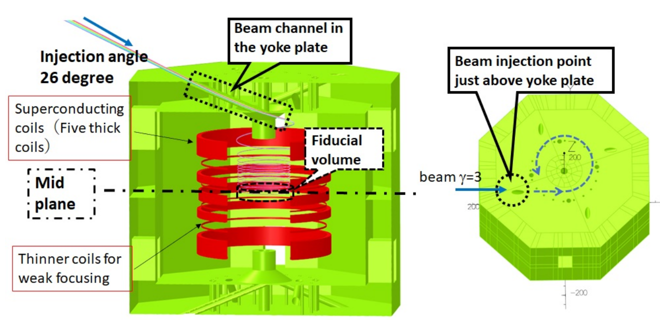

Fig. 2. Superconducting solenoid magnet for this experiment [1], [3].

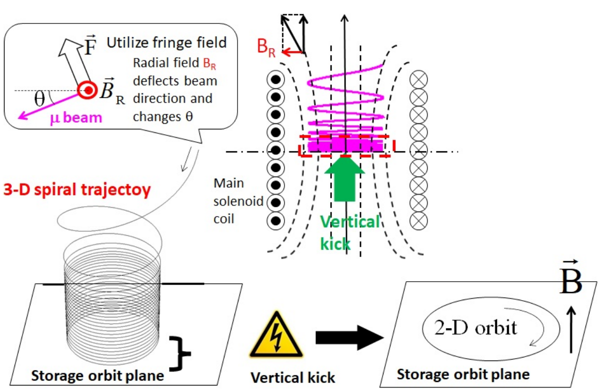

Fig. 3. Outline of three-dimensional beam injection scheme [4].

the smallest storage ring for relativistic energy beam in the world, and will allow us to accomplish (ii) introduced in the previous section. In order to realize (i) and (iii), a brand-new beam injection scheme named as **Three-dimensional spiral injection scheme** as shown in Fig 3 has been developed [4]. The beam enters the solenoid through a channel in the top iron yoke 110 cm above of the storage volume (see Fig. 2), and its spiral motion is compressed by the Fleming force due to static radial field ($\vec{B_R}$). A vertical kick (pulsed radial magnetic field) is applied to store the beam, when the beam arrives the storage region. A very small static weak-focusing field in the fiducial volume maintains the beam in the storage region. No electric field is required in this injection scheme which meets requirement of (i).

III. X-Y COUPLING FOR THE THREE DIMENSIONAL SPIRAL BEAM INJECTION SCHEME

Because solenoid magnet has axis-symmetric field distribution, the muon beam phase space is required to have dedicated treatments at the beam injection point. If we take the beam direction as Z-axis, transverse beam motion in X-Y plane should be coupled with appropriate correlations (**X-Y coupling**) to compensate axis-symmericity of solenoidal magnetic field distribution. Fig. 4 is a comparison of trajectories without/with applying X-Y coupling. Beam cross-section views at the injection are also shown. It is clear that vertical size of the stored beam is controlled by X-Y coupling.

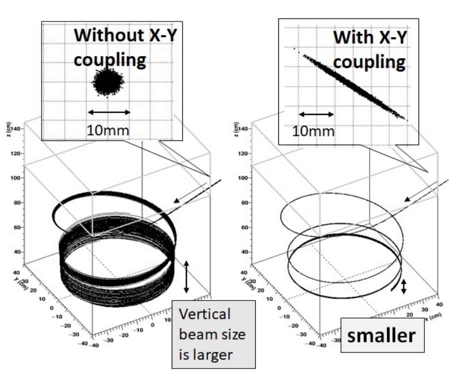

Fig. 4. X-Y coupling dependence on three-dimensional trajectory.

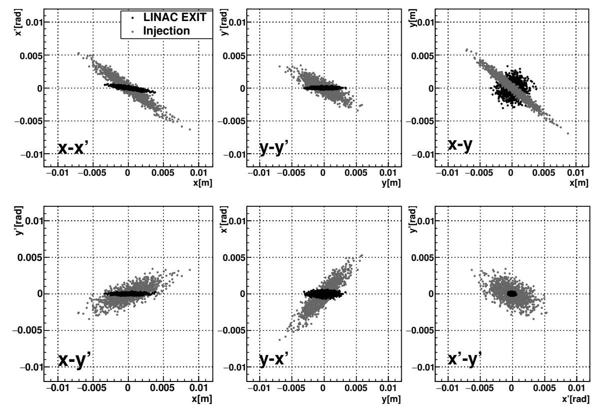

Fig. 5. Beam phase spaces with strong X-Y coupling (gray) and without (black) are shown.

TABLE I
A LIST OF BEAM PARAMETERS FOR THE BEAM TRANSPORT LINE

Twiss parameters /position	α_x	β_x	α_y	β_y
LINAC EXIT	0	10	0	10
Injection	9.29	10	6.99	10
Extended Twiss /position	r_1	r_2	r_3	r_4
LINAC EXIT	0	0	0	0
Injection	0.6	-0.45	-1.3	-1.3

To describe a state of a particle, a four-dimensional phase space as in Fig. 5 is convenient. Nevertheless, the knowledge of these coordinates for each single particle represent too much information, so that only the envelope of the beam is represented in the phase space. In practice, the canonical form chosen would be an ellipse and its representation by the so-called sigma-matrix as in Eq. 4 is often used. Components of diagonal block matrix are related with Twiss-parameters as $\alpha_x = -\langle xx' \rangle/\epsilon_x$, $\beta_x = \langle x^2 \rangle/\epsilon_x$, and $\epsilon_x = \sqrt{\langle x^2 \rangle\langle x'x' \rangle - \langle xx' \rangle^2} = 1.5 \times 10^{-6} rad \cdot m$. (The same for Y-components.) Other correlated components of $\langle xy \rangle$, $\langle x'y \rangle$, $\langle yx' \rangle$ and $\langle x'y' \rangle$ are related with Extended-Twiss parameters. We estimate Twiss parameters from Fig. 5 and summarize in Table I.

$$\sigma^{4D} = \begin{bmatrix} \langle x^2 \rangle & \langle xx' \rangle & \langle xy \rangle & \langle xy' \rangle \\ \langle xx' \rangle & \langle x'^2 \rangle & \langle x'y \rangle & \langle x'y' \rangle \\ \langle yx \rangle & \langle yx' \rangle & \langle y^2 \rangle & \langle yy' \rangle \\ \langle y'x \rangle & \langle y'x' \rangle & \langle y'y \rangle & \langle y'^2 \rangle \end{bmatrix} \tag{4}$$

In order to apply appropriate X-Y coupling on the beam phase space, we designed a transport line which satisfies transfer matrix M:

$$\sigma_0^{4D} = M^t \sigma_1^{4D} M \tag{5}$$

here, we write sigma-matrix at the exit of the LINAC (σ_0^{4D}) and at injection point (σ_1^{4D}). α and β in Table I are controlled by *Normal* magnets, while $r_1 - r_4$ are controlled by magnets with skew of *Rotating angle* ϕ as in Fig. 6.

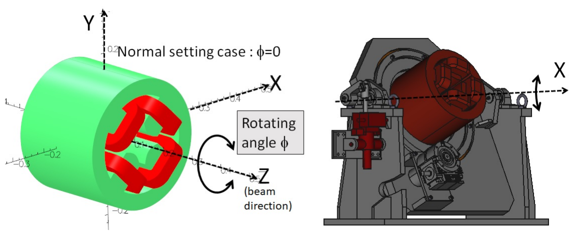

Fig. 6. Left:Three-dimensional model design of quadruple is shown. Definitions of rotating angle ϕ and *normal* is also shown. Right:Drawing of a dedicated support system to adjust pitch and rotating angles.

TABLE II
A LIST OF QUADRUPLE MAGNETS FOR THE BEAM TRANSPORT LINE

ID	Bore radius [mm]	K [T/m]	Effective length [m]	angle ϕ (DEG)
Q1	10	-18.1	0.25	0
Q2	10	17.4	0.25	0
Q3	10	-17.6	0.25	0
Q4	10	-20.2	0.29	-30.6
Q5	10	3.7	0.29	38.7
Q6	30	0.71	0.29	28.4
Q7	30	0.64	0.29	32.8
Q8	30	1.04	0.29	28.9
Q9	30	-0.64	0.29	-36.8
Q10	30	-2.31	0.29	31.8

IV. Design of Beam Transport Line for Required Transfer Matrix

Fig. 7 shows an image of the entire beam line at J-PARC MUSE. As described in Fig. 2, pitch angle through the iron channel at the injection point, is 26 degrees from the fringe field $\vec{B}_R$ of the storage magnet. Vertical level at the injection point is, therefore, 4 m below the LINAC beam line level. 3.5 m drift space is set just upstrem of the injection point to meet requirement the storage magnet. Two vertical dipole magnets bend a beam direction by 13 degrees for each, and three *normal* quadruple magnets are set between the two dipole magnets in order to control the vertical energy-dispersion function (η_y) as minimize as possible.

Seven *rotating* quadruple magnets will control X-Y coupling at the injection point. Entire transfer matrix M of the transport line as in Eq. 5 can be disassembled every matrix along the beam line components (drift-space, dipoles and quadruples).

Now we introduce how to control X-Y coupling with arbitrary rotating quadruples. Rotating matrix of arbitrary angle ϕ is written as:

$$R(\phi) = \begin{bmatrix} \cos\phi & 0 & \sin\phi & 0 \\ 0 & \cos\phi & 0 & \sin\phi \\ -\sin\phi & 0 & \cos\phi & 0 \\ 0 & -\sin\phi & 0 & \cos\phi \end{bmatrix}, \qquad (6)$$

in case of six rotating magnets, we introduce **R-matrix**:

$$R = \begin{bmatrix} \mu & 0 & -r_1 & r_2 \\ 0 & \mu & r_3 & r_4 \\ r_1 & r_2 & 0 & \mu \\ r_3 & r_4 & 0 & 0 \end{bmatrix}, \qquad (7)$$

here $\mu = \sqrt{1 - det(R)}$ and $det(R) = r_1 r_4 - r_2 r_3$.

Entire transfer matrix M is disassembled with diagonal block matrix D and R-matrix as:

$$M = R^{-1} D. \qquad (8)$$

Diagonal block matrix D is estimated Twiss-parameters in Table I. The matrix R includes four independent parameters ($r_1 - r_4$) in Table I, too. We use SAD [5] as a tool for detailed design of each component of the transport line. Table II is an output of SAD: a list of quadruple magnets in the transport line. Fig. 8 and 9 are simulated beam size along the beam transport line. Bore radius in Table II is decided from these beam size simulation. Technical difficulties of beam transport design are to keep transverse beam size smaller and to adjust total path length including 3.5 m driftspace to given number from the bulding design.

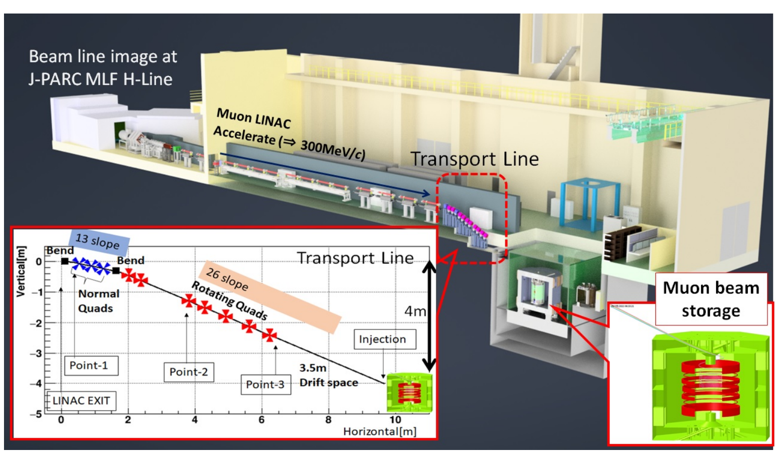

Fig. 7. An image of the entire beam line at J-PARC MUSE. Pitch angle is 26 degrees, and a vertical level at the injection point is 4 m below from the LINAC beam line height. Special support system for magnets on such steep beam line is required as in Fig. 6.

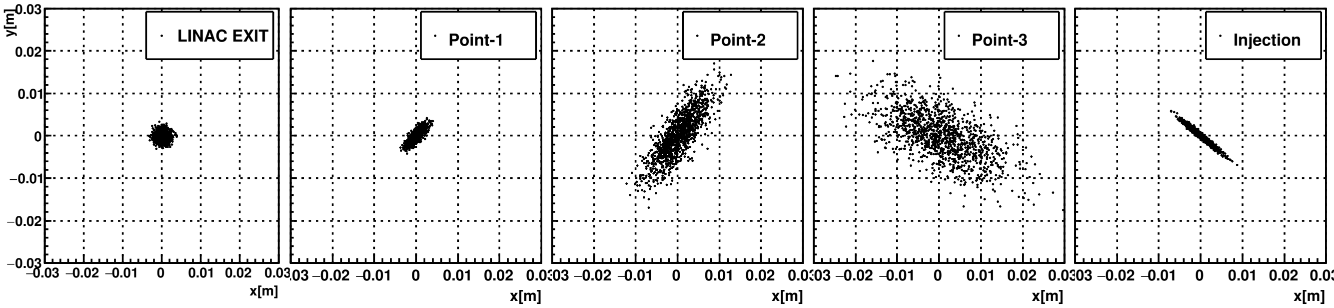

Fig. 8. Transverse beam cross-section views at different points along the transport line. Beam size at point-3 is the biggest due to to apply strong focus on the injection point beyond the 3.5 m drift space.

V. η_y DEPENDENCE ON THE TRANSVERSE BEAM SIZE

Fig. 9 shows vertical energy distribution η_y as a function of path length s [m] of the transport line, as well as $det(R)$. Two of vertical dipoles tend to generate vertical energy dispersionη_y. Therefore, we study how well we should control η_y to minimize transverse beam size along the transport line. ID-0 does not care to control η_y. ID-1 and ID-2 care to set $\eta_y = 0$ and $\eta_y^{'} = 0$ by use of Q1 – Q3, between the two dipoles. It is obvious that transverse beam RMS sizes, σ_x and σ_y in Fig. 9, depend on how well we control η_y from comparison of three cases:ID-0, ID-1 and ID-2.

$det(R)$ is also important to set realistic beam line parameters. If $det(R) > 1$, μ in Eq. 7 becomes imaginary number, and realistic transport line is not applicable. SAD allow $det(R)$ less than 0.65 for reasonably stable X-Y coupling along the beam line [5]. Depends on Twiss parameter at the second dipole magnet, beam sizes of downstream do change. A difference between ID-1 and ID-2 comes from different β_x at the second dipole magnet.

Finally, ID-2 would be better as final decision. As in Fig 8, transverse beam size along the transport line is below 10 mm-RMS. Typical cross-section views at different five points are also shown in Fig. 9. Based on these studies, we decide radius of beam pipes and bore radius of quadruples and gap distance of dipole magnets as in Table II. Detailed three-dimensional magnetic field design towards fabrication of these quadruples is ongoing by use of OPERA-3D and will be completed in few months.

VI. SUMMARY AND FUTURE

In this paper, a strategy to design of a dedicated beam transport line for J-PARC Muon g-2/EDM experiment is described. Three important technical requirements for the new experiment are introduced. A strong X-Y coupling is a key to meet requirement and to accomplish three-dimensional spiral injection scheme. Transfer matrix of the beam transport line is introduced and detail parameters of ten quadruple magnets along the transport line are presented. Further study to investigate muon beam momentum dispersion ($\Delta p/p$) to the X-Y coupling will be reflected to the final transport line design.

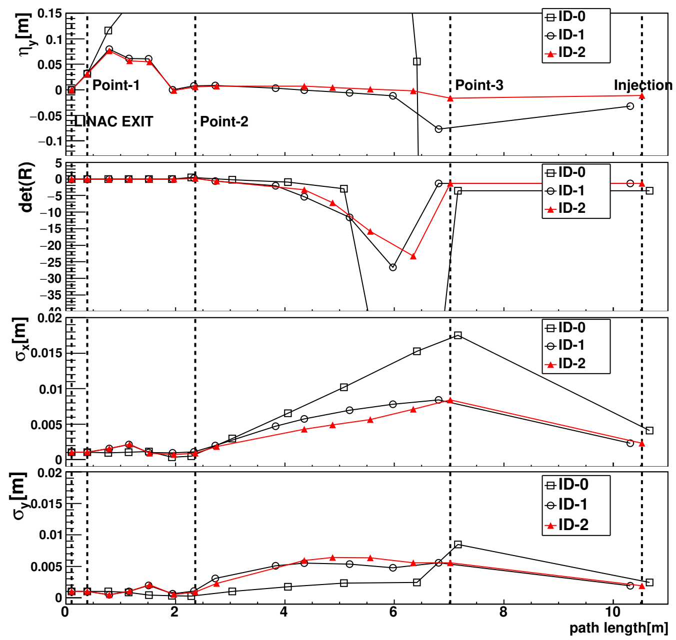

Fig. 9. η_y as a function of path length s [m], as well as $det(R)$ is shown. RMS beam sizes σ for both X and Y components are smaller than 10 mm.

A design work for dedicated support system to apply arbitrary rotating angle (for Q4 – Q10) is in progress.

As already shown in Fig. reffig6, an image of current ongoing design which is designed to have tilt angle is 26 degrees. We are working on one set of quadruple fabrication by the end of FY 2021. Successive construction works will be continued towards complete the beam transport line completion by FY2026.

ACKNOWLEDGMENT

H.Iinuma thanks…Prof. K.Oide for beneficial suggestions.

REFERENCES

[1] M. Abe and J-PARC g-2/EDM Collaboration, "A new approach for measuring the muon anomalous magnetic moment and electric dipole moment", Prog. Theor. Exp. Phys. 2019, 053C02, 2019.

[2] G. W. Bennett et al. (Muon (g-2) Collaboration) ”Improved limit on the muon electric dipole moment” Physical Review D 80, 052008, 2009. DOI:https://doi.org/10.1103/PhysRevD.80.052008

[3] M. Abe, Y. Murata, H. Iinuma, T. Ogitsu, N. Saito, K. Sasaki, T. Mibe, H. Nakayama, ”Magnetic design and method of a superconducting magnet for muon g-2 /EDM precise measurements in a cylindrical volume with homogeneous magnetic field”, Nuclear Inst. and Methods in Physics Research, A: Vol. 890, 2018, PP. 51-63.

[4] H. Iinuma, H. Nakayama, K. Oide, K. Sasaki, N. Saito, T. Mibe, M. Abe, ”Three-dimensional spiral injection scheme for g-2/EDM experiment at J-PARC”, Nuclear Instruments and Methods in Physics Research A, 832, 2016, pp51-62.

[5] https://acc-physics.kek.jp/SAD/